

Effect of graded interphase on the coefficient of thermal expansion for composites with spherical inclusions

Roberta Sburlati

Department of Civil, Chemical and Environmental Engineering (DICCA)

University of Genova, Via Montallegro 1, 16145 Genova, Italy

E-mail: roberta.sburlati@unige.it

Maria Kashtalyan

Centre for Micro- and Nanomechanics (CEMINACS),

School of Engineering, University of Aberdeen, Scotland UK

E-mail: m.kashtalyan@abdn.ac.uk

Roberto Cianci

DIME - Sez. Metodi e Modelli Matematici

University of Genova, Piazzale Kennedy, pad.D, 16129 Genova, Italy

E-mail: roberto.cianci@unige.it

December 19, 2016

Abstract

The paper is concerned with the quantitative characterisation of the effective coefficient of thermal expansion for a particulate composite containing spherical inclusions surrounded by an interphase zone, whose properties are graded in the radial direction. A thermo-elastic problem of uniform heating is studied for a single hollow spherical inclusion embedded in a finite matrix assuming power-law variation of the thermo-elastic

properties. An exact solution of the problem is derived using hypergeometric functions. The effective coefficient of thermal expansion is determined in closed form for composites with graded interphase zone around hollow and solid inclusions, as well as for the case of void in a graded matrix. Numerical results highlighting the effect of the interphase properties on the coefficient of thermal expansion for different volume fractions of inclusions are presented and discussed.

Keywords: Elasticity; Particle reinforced composites; Thermal properties; Spherical inclusions.

1 Introduction

Properties of particulate composite materials are greatly affected by the degree of adhesion at the interface between inclusions and the matrix, as is often evidenced by experimental observations. The mismatch of properties between the composite's phases may lead to creation of microcracks, impurities, local porosities and stress concentrations around inclusions.

To describe the effect of these phenomena on composite's properties, a number of different micromechanical models have been proposed in the literature, with some authors introducing an interphase zone between inclusions and the matrix, with properties that differ from those of both main phases.

For spherical inclusions and all phases being homogeneous isotropic, experimental results showed, in particular for polymeric materials and concrete, that properties of the interphase zone are not uniform but vary radially outward from the centre of the inclusion (i.e. Holliday and Robinson, 1973; Sideridis and Papanicolau, 1988; Lutz et al, 1997). A number of researchers adopted this model and tried to predict the mechanical properties of particulate composites, assuming a specific profile for the properties of the interphase zone and employing various methods.

In 1991, Hashin proposed a three-phase sphere model (Hashin, 1991) which assumes a thin interphase zone surrounding each inclusion, with uniform elastic properties that are different

from the properties of both matrix and inclusion. He proposed replacement technique to calculate the properties depending on the volume fraction of inclusions. Several authors have extended this method to the graded interphase zone; this was done by subdividing the interphase zone into a number of concentric homogeneous layers, each having different properties, and using them to simulate a specific profile of the graded interphase (n-layered sphere model) (Herve, 2002; Lombardo, 2005; Gusev, 2014).

A different methodology was proposed by Shen and Li (2003, 2005). The authors adopted an effective interphase model (EIM) and a uniform replacement model (URM) to study the effect of an homogeneous interphase with elastic properties that vary in radial direction. The basic idea of this approach is to replace the inclusion with its surrounding multi-layered interphase with a homogeneous inclusion and to increase the thickness of the interphase in an incremental, differential manner with homogenisation at each step. Sevostianov and Kachanov (2007) utilized the Shen and Li's methodology to study the effect of interphase layers on the overall elastic and conductive properties of matrix composite and introduced modifications to the previous methodology to better describe composites with nanoinclusions.

In 1996, Lutz and Zimmerman proposed to model the interphase zone around an inclusion as a matrix material with properties that vary in the radial direction according to the power law and asymptotically approach the value of the homogeneous matrix at infinity (Lutz and Zimmerman, 1996). Later, Zimmerman and Lutz (1999), studied thermo-mechanical problems in an uniformly-heated functionally-graded cylinder. They were the first to show that thermo-mechanical-problems involving radially inhomogeneous materials could be solved using hypergeometric functions.

Adopting Lutz and Zimmerman's interphase model, Sburlati and Cianci (2015) determined the bulk modulus of particulate composites with solid and hollow spherical inclusions. A closed-form solution was obtained using hypergeometric functions, and an explicit expression for the effective bulk modulus was obtained following (Christensen, 2005). A detailed parametric investigation of this expression for non-dilute inclusions was presented in (Sburlati and Monetto, 2016).

In the present paper, we study the effect of size and properties of the interphase zone on the coefficient of thermal expansion (CTE). CTE plays a critical role in design of composite materials for extreme thermal environments (Sevostianov, 2011). The paper approaches the problem of determining CTE along the lines developed in the previous work by the authors (Sburlati and Cianci, 2015). However, in order to explore the influence of the size of the interphase zone, we consider the graded interphase zone of finite size, with thermo-elastic properties that vary according to the power law and match properties of the matrix at its interface with the matrix, while remaining distinct from the properties of the inclusion at its interface with the inclusion. In the last aspect, the graded interphase model used in the present paper differs from the graded interlayers investigated by the authors previously (Kashtalyan et al, 2009; Sburlati and Kashtalyan, 2016), the properties of which exactly match those of adjacent layers.

To this end, a single composite sphere of a particulate composite with hollow spherical inclusions is considered. The exact analytical solution to the thermo-elasticity problem of uniform heating is derived using hypergeometric function theory (Erdelyi et al, 1953). The exact CTE expressions are obtained for solid and hollow inclusions in terms of the interphase zone properties and inclusion volume fraction following (Christensen, 2005).

The obtained solution can be also used to describe voids with imperfect interfaces in porous materials (Hatta et al, 2010), two-phase composites with graded inclusions (Lombardo, 2005) and thin-walled hollow inclusions with damages in their walls, i.e. syntactic foams (Tagliavia et al, 2010).

When the properties at the interface with the inclusion are taken equal to the properties of the matrix, the exact expression for the CTE obtained in the present paper approaches the CTE expression obtained by Levin (1967) for a composite with two homogeneous phases.

Numerical results for solid inclusions, hollow inclusions and voids, at a range of phase volume fractions, are presented, and the effects of size and properties of the interphase zone on the CTE are established and discussed.

It is important to emphasise that recent interest to such models is triggered not only

by desire to predict the effective properties of particulate composites more accurately, but also by the drive to improve performance of nanocomposites, in which thin inhomogeneous coatings around nanoparticles can be used to increase thermo-mechanical properties of the nanocomposites. It was shown that for nanocomposites thin coatings at the interfaces between constituents of a composite material can make a substantial difference to their functional characteristics and reliability (Sevostianov and Kachanov, 2006; Zappalorto et al, 2011; Anisimova et al, 2016).

2 Problem formulation

Figure 1 shows a single hollow composite sphere embedded in a finite matrix, in according to describe the composite spheres model for a nondilute elastic suspension of spherical particles (Hashin, 1962; Christensen, 2005; Nemat-Nasser, 1993). Let the outer radius of the composite sphere be R , and the inner and outer radii of the inclusion be a and b . In this way, a solid inclusion and a void can be viewed as particular cases of a hollow inclusion, when $a = 0$ and $a = b$ respectively. The solution for a void in a matrix may be also adopted to describe a two-phase composite sphere with a functionally graded hollow spherical inclusion.

The inclusion and the matrix are assumed to be homogeneous isotropic, and referred to a spherical co-ordinate system $(0; r, \theta, \phi)$. The elastic properties of the inclusion are denoted as λ_i, μ_i , while the coefficient of thermal expansion (CTE) as α_i . Corresponding properties of the matrix are denoted λ_m, μ_m and α_m .

In order to investigate the interphase zone between the inclusion and the matrix, let us introduce a layer of radius c around the spherical inclusion. We assume that the elastic and thermal properties of this layer vary in the radial direction, exactly matching properties of the matrix, in which the inclusion is embedded, at the interface $r = c$. At the same time, the interface $r = b$ between the inclusion and the interphase zone remains distinct and clearly defined. The elastic and thermal properties of the interphase zone at $r = b$ are denoted as λ_{ip}, μ_{ip} and α_{ip} . The elastic and thermal properties of the interphase zone at its interface

with the matrix are the same as those of the matrix.

Assuming power-law variation in the radial direction, the elastic and thermal properties of the graded interphase zone are described as follows

$$\lambda(r) = \lambda_1 + \lambda_2 \left(\frac{b}{r}\right)^\beta, \quad \mu(r) = \mu_1 + \mu_2 \left(\frac{b}{r}\right)^\beta, \quad \alpha(r) = \alpha_1 + \alpha_2 \left(\frac{b}{r}\right)^\beta, \quad (2.1)$$

where

$$\begin{aligned} \lambda_1 &= \frac{b^\beta \lambda_{ip} - c^\beta \lambda_m}{b^\beta - c^\beta}, & \lambda_2 &= \frac{c^\beta (\lambda_m - \lambda_{ip})}{b^\beta - c^\beta}, \\ \mu_1 &= \frac{b^\beta \mu_{ip} - c^\beta \mu_m}{b^\beta - c^\beta}, & \mu_2 &= \frac{c^\beta (\mu_m - \mu_{ip})}{b^\beta - c^\beta}, \end{aligned} \quad (2.2)$$

$$\alpha_1 = \frac{b^\beta \alpha_{ip} - c^\beta \alpha_m}{b^\beta - c^\beta}, \quad \alpha_2 = \frac{c^\beta (\alpha_m - \alpha_{ip})}{b^\beta - c^\beta},$$

and

$$\begin{aligned} \lambda_{ip} &= \lambda(b), & \mu_{ip} &= \mu(b), & \alpha_{ip} &= \alpha(b), \\ \lambda_m &= \lambda(c), & \mu_m &= \mu(c), & \alpha_m &= \alpha(c). \end{aligned} \quad (2.3)$$

The inhomogeneity parameter β control the profile of the power law associated with the graded interphase zone; we assume that it is the same for elastic and for thermal properties since we suppose that the same physical inhomogeneity will control both the thermal and the mechanical behaviour.

When the interphase zone is absent, we have: $\lambda_1 = \lambda_m$, $\mu_1 = \mu_m$, $\alpha_1 = \alpha_m$ and $\lambda_2 = \mu_2 = \alpha_2 = 0$.

We remark that, at the external radius $r = c$ of the finite interphase region, we exactly match the mechanical and thermal properties of the sphere with the mechanical and thermal properties of the matrix. The radius $R > c$, which disappears in the final results, plays essentially only an auxiliary role limiting the single composite sphere where we are working.

In order to obtain the thermoelasticity solution needed for determination of the CTE, we study a thermoelastic problem of the composite sphere subjected to a uniform temperature T . We assume that the inner $r = a$ and the outer $r = R$ boundaries are stress free

$$\sigma_r^{(i)}(a) = 0, \quad \sigma_r^{(m)}(R) = 0. \quad (2.4)$$

and that perfect bonding exists at all interfaces, therefore continuity conditions for the radial stress and displacement are satisfied at the interface between the interphase zone and inclusion $r = b$ and the interphase zone and matrix $r = c$

$$\begin{aligned}\sigma_r^{(i)}(b) &= \sigma_r^{(ip)}(b), & u^{(i)}(b) &= u^{(ip)}(b), \\ \sigma_r^{(ip)}(c) &= \sigma_r^{(m)}(c), & u^{(ip)}(c) &= u^{(m)}(c).\end{aligned}\tag{2.5}$$

3 Governing equations

In this section, we derive the exact solution to the thermoelasticity problem of the composite sphere (Figure 1) undergoing an isothermal radially symmetric deformation due to a uniform temperature T .

Since the deformation is radially symmetric, the strain-displacement relations are

$$\epsilon_r(r) = \frac{du(r)}{dr}, \quad \epsilon_\theta(r) = \epsilon_\phi(r) = \frac{u(r)}{r},\tag{3.1}$$

and the equilibrium equation have the form

$$\frac{d\sigma_r(r)}{dr} + \frac{2\sigma_r(r) - \sigma_\theta(r) - \sigma_\phi(r)}{r} = 0.\tag{3.2}$$

The Duhamel-Neumann constitutive relations for radially inhomogeneous material undergoing radially symmetric deformation are given by (Love, 1944) as

$$\begin{aligned}\sigma_r(r) &= 2\mu(r)\epsilon_r(r) + \lambda(r)(\epsilon_r(r) + \epsilon_\theta(r) + \epsilon_\phi(r)) - (3\lambda(r) + 2\mu(r))\alpha(r)(T - T_0), \\ \sigma_\theta(r) = \sigma_\phi(r) &= 2\mu(r)\epsilon_\theta(r) + \lambda(r)(\epsilon_r(r) + \epsilon_\theta(r) + \epsilon_\phi(r)) - (3\lambda(r) + 2\mu(r))\alpha(r)(T - T_0),\end{aligned}\tag{3.3}$$

where T_0 is the reference uniform temperature at which the solid is stress free when all external forces are zero.

Given that Lamé moduli and the thermal expansion coefficients were defined as (2.1) and (2.2), the thermo-elastic equation in terms of displacements takes the form

$$\begin{aligned}\left(\left(\frac{r}{b}\right)^\beta - L\right)\frac{d^2u}{dr^2} + \left(2\left(\frac{r}{b}\right)^\beta + (\beta - 2)L\right)\frac{1}{r}\frac{du}{dr} - \left(2\left(\frac{r}{b}\right)^\beta - NL\right)\frac{u}{r^2} + \\ + \left(\left(\frac{b}{r}\right)^\beta g_1 + g_2\right)\frac{L}{r}(T - T_0) = 0,\end{aligned}\tag{3.4}$$

where

$$L = -\frac{\lambda_2 + 2\mu_2}{\lambda_1 + 2\mu_1}, \quad N = \frac{2(\lambda_2(\beta + 1) + 2\mu_2)}{\lambda_2 + 2\mu_2},$$

$$g_1 = -\frac{2(3\lambda_2 + 2\mu_2)\alpha_2\beta}{\lambda_2 + 2\mu_2}, \quad g_2 = -\frac{(3\lambda_2 + 2\mu_2)\alpha_1\beta}{\lambda_2 + 2\mu_2} - \frac{(3\lambda_1 + 2\mu_1)\alpha_2\beta}{\lambda_2 + 2\mu_2}. \quad (3.5)$$

When $L = 0$, the equation (3.4) reduces to that for a homogeneous material.

4 Solution method

The solution of the equation (3.4) is sought in the following form (Sburlati et al, 2015; Erdelyi et al, 1953)

$$u(r) = \left(\frac{A_1}{r^2} \Theta_1(r) + A_2 r \Theta_2(r) + \left(g_3 - \frac{g_4}{r^\beta} \right) r \right) (T - T_0) \quad (4.1)$$

Here A_1 and A_2 are two unknown constants, and

$$g_3 = \frac{((\lambda_2 + 2\mu_2)(3\lambda_2 + 2\mu_2)\alpha_1 + 4(\lambda_1\mu_2 - \lambda_2\mu_1)\alpha_2)\beta}{(3\lambda_2 + 2\mu_2)((\lambda_2 + 2\mu_2)\beta - (3\lambda_2 + 4\mu_2))} +$$

$$-\frac{(3\lambda_2 + 4\mu_2)(3\lambda_2 + 2\mu_2)\alpha_1 + 2(\mu_2(3\lambda_1 - 2\mu_1) - 6\lambda_2\mu_1)\alpha_2}{(3\lambda_2 + 2\mu_2)((\lambda_2 + 2\mu_2)\beta - (3\lambda_2 + 4\mu_2))}, \quad (4.2)$$

$$g_4 = \frac{(3\lambda_2 + 2\mu_2)\alpha_2 b^\beta}{(\lambda_2 + 2\mu_2)\beta - (3\lambda_2 + 4\mu_2)}.$$

The hypergeometric functions $\Theta_1(r)$ and $\Theta_2(r)$ are written as (Abramovitz, 1965)

$$\Theta_1(r) = {}_2F_1\left(\frac{1}{2} - G + \frac{3}{2\beta}, \frac{1}{2} + G + \frac{3}{2\beta}; 1 + \frac{3}{\beta}; \frac{b^\beta}{r^\beta} L\right),$$

$$\Theta_2(r) = {}_2F_1\left(\frac{1}{2} + G - \frac{3}{2\beta}, \frac{1}{2} - G - \frac{3}{2\beta}; 1 - \frac{3}{\beta}; \frac{b^\beta}{r^\beta} L\right), \quad (4.3)$$

where

$$G = \frac{1}{2} \sqrt{1 - \frac{2}{\beta} + \frac{4N+1}{\beta^2}}. \quad (4.4)$$

From equations (3.3), (2.1) and (4.1), the stresses are

$$\begin{aligned}
\frac{\sigma_r(r)}{T-T_0} = & \left((\lambda_1 + 2\mu_1 + (\lambda_2 + 2\mu_2) b^\beta r^{-\beta}) q_1 b^\beta \beta r^{-(3+\beta)} \Theta_3(r) - 4 (\mu_1 + \mu_2 b^\beta r^{-\beta}) r^{-3} \Theta_1(r) \right) A_1 + \\
& + \left((3\lambda_1 + 2\mu_1 + (3\lambda_2 + 2\mu_2) b^\beta r^{-\beta}) \Theta_2(r) + (\lambda_1 + 2\mu_1 + (\lambda_2 + 2\mu_2) b^\beta r^{-\beta}) q_2 b^\beta \beta r^{-\beta} \Theta_4(r) \right) A_2 + \\
& + (3\lambda_1 + 2\mu_1 + (3\lambda_2 + 2\mu_2) b^\beta r^{-\beta}) g_3 - (3\lambda_1 + 2\mu_1 + (3\lambda_2 + 2\mu_2) b^\beta r^{-\beta}) (\alpha_1 + \alpha_2 b^\beta r^{-\beta}) + \\
& + \left((\lambda_1 + 2\mu_1 + (\lambda_2 + 2\mu_2) b^\beta r^{-\beta}) \beta - (3\lambda_1 + 2\mu_1) - (3\lambda_2 + 2\mu_2) b^\beta r^{-\beta} \right) r^{-\beta} g_4, \\
\\
\frac{\sigma_\theta(r)}{T-T_0} = & \left((\lambda_1 + \lambda_2 b^\beta r^{-\beta}) q_1 b^\beta \beta r^{-(3+\beta)} \Theta_3(r) + 2 (\mu_1 + \mu_2 b^\beta r^{-\beta}) r^{-3} \Theta_1(r) \right) A_1 + \\
& + \left((3\lambda_1 + 2\mu_1 + (3\lambda_2 + 2\mu_2) b^\beta r^{-\beta}) \Theta_2(r) + (\lambda_1 + \lambda_2 b^\beta r^{-\beta}) q_2 b^\beta \beta r^{-\beta} \Theta_4(r) \right) A_2 + \\
& + (3\lambda_1 + 2\mu_1 + (3\lambda_2 + 2\mu_2) b^\beta r^{-\beta}) g_3 - (3\lambda_1 + 2\mu_1 + (3\lambda_2 + 2\mu_2) b^\beta r^{-\beta}) (\alpha_1 + \alpha_2 b^\beta r^{-\beta}) + \\
& + \left((\lambda_1 + \lambda_2 b^\beta r^{-\beta}) \beta - (3\lambda_1 + 2\mu_1) - (3\lambda_2 + 2\mu_2) b^\beta r^{-\beta} \right) r^{-\beta} g_4,
\end{aligned} \tag{4.5}$$

where

$$q_1 = \frac{4\mu_2}{(\lambda_1 + 2\mu_1)(\beta + 3)}, \quad q_2 = -\frac{3\lambda_2 + 2\mu_2}{(\lambda_1 + 2\mu_1)(\beta - 3)}, \tag{4.6}$$

for $\beta \neq 3$ and

$$\begin{aligned}
\Theta_3(r) &= {}_2F_1 \left(\frac{3}{2} - G + \frac{3}{2\beta}, \frac{3}{2} + G + \frac{3}{2\beta}; 2 + \frac{3}{\beta}; \frac{b^\beta}{r^\beta} L \right), \\
\Theta_4(r) &= {}_2F_1 \left(\frac{3}{2} - G - \frac{3}{2\beta}, \frac{3}{2} + G - \frac{3}{2\beta}; 2 - \frac{3}{\beta}; \frac{b^\beta}{r^\beta} L \right).
\end{aligned} \tag{4.7}$$

We recall that

$$\frac{d}{dr} \Theta_1(r) = \frac{q_1 b^\beta \beta \Theta_3(r)}{r^{\beta+1}}, \quad \frac{d}{dr} \Theta_2(r) = \frac{q_2 b^\beta \beta \Theta_4(r)}{r^{\beta+1}}. \tag{4.8}$$

The analytical solution (4.1) and (4.5) is applicable to the graded interphase zone of Figure 1.

For homogeneous material, the Navier equation (3.4) takes the usual form

$$\frac{d^2 u(r)}{dr^2} + \frac{2}{r} \frac{du(r)}{dr} - \frac{2u(r)}{r^2} = 0. \tag{4.9}$$

For the inclusion, the solution of this equation is written as

$$\begin{aligned}
u^{(i)}(r) &= \left(\frac{B_1}{r^2} + B_2 r \right) (T - T_0), \\
\sigma_r^{(i)}(r) &= \left(-\frac{4\mu_i B_1}{r^3} + (3\lambda_i + 2\mu_i) B_2 - (3\lambda_i + 2\mu_i) \alpha_i \right) (T - T_0), \\
\sigma_\theta^{(i)}(r) &= \left(\frac{2\mu_i B_1}{r^3} + (3\lambda_i + 2\mu_i) B_2 - (3\lambda_i + 2\mu_i) \alpha_i \right) (T - T_0).
\end{aligned} \tag{4.10}$$

Similarly, for the matrix it is written as

$$\begin{aligned}
u^{(m)}(r) &= \left(\frac{C_1}{r^2} + C_2 r \right) (T - T_0), \\
\sigma_r^{(m)}(r) &= \left(-\frac{4\mu_m C_1}{r^3} + (3\lambda_m + 2\mu_m) C_2 - (3\lambda_m + 2\mu_m) \alpha_m \right) (T - T_0), \\
\sigma_\theta^{(m)}(r) &= \left(\frac{2\mu_m C_1}{r^3} + (3\lambda_m + 2\mu_m) C_2 - (3\lambda_m + 2\mu_m) \alpha_m \right) (T - T_0).
\end{aligned} \tag{4.11}$$

When the interphase zone is absent, the solutions (4.1) and (4.5) reduce to that for the homogeneous material. Actually, in this case we have $q_1 = q_2 = 0$, $g_4 = 0$ and $L = 0$, which in turn implies $\Theta_i(r) = 1$ for $i = 1, 2, 3, 4$.

To determine the six unknown constants A_1, A_2, B_1, B_2, C_1 and C_2 in equations (4.1), (4.5), (4.10) and (4.11), we employ the boundary and interface conditions (2.4) and (2.5).

The constants are found explicitly as

$$\begin{aligned}
B_1 &= \frac{(3\lambda_i + 2\mu_i) a^3 (\Theta_1(b) A_1 + b^3 \Theta_2(b) A_2)}{4b^3 \mu_i + (3\lambda_i + 2\mu_i) a^3} + \\
&\quad - \frac{(3\lambda_i + 2\mu_i) a^3 b^3 (b^{-\beta} g_4 - g_3)}{4b^3 \mu_i + (3\lambda_i + 2\mu_i) a^3} - \frac{(3\lambda_i + 2\mu_i) \alpha_i a^3 b^3}{4b^3 \mu_i + (3\lambda_i + 2\mu_i) a^3}, \\
B_2 &= \frac{4\mu_i (\Theta_1(b) A_1 + b^3 \Theta_2(b) A_2)}{4b^3 \mu_i + (3\lambda_i + 2\mu_i) a^3} + \frac{4\mu_i b^3 (g_3 - b^{-\beta} g_4)}{4b^3 \mu_i + (3\lambda_i + 2\mu_i) a^3} + \\
&\quad + \frac{(3\lambda_i + 2\mu_i) \alpha_i a^3}{4b^3 \mu_i + (3\lambda_i + 2\mu_i) a^3},
\end{aligned} \tag{4.12}$$

$$C_1 = \frac{(3\lambda_m + 2\mu_m)R^3(\Theta_1(c)A_1 + \Theta_2(c)c^3A_2)}{R^3(3\lambda_m + 2\mu_m) + 4c^3\mu_m} + \frac{(3\lambda_m + 2\mu_m)R^3c^3(c^{-\beta}g_4 - g_3)}{R^3(3\lambda_m + 2\mu_m) + 4c^3\mu_m} - \frac{(3\lambda_m + 2\mu_m)R^3c^3\alpha_m}{R^3(3\lambda_m + 2\mu_m) + 4c^3\mu_m}, \quad (4.13)$$

$$C_2 = \frac{4\mu_m(\Theta_1(c)A_1 + \Theta_2(c)c^3A_2)}{(3\lambda_m + 2\mu_m)R^3 + 4c^3\mu_m} - \frac{4c^3\mu_m(c^{-\beta}g_4 - g_3)}{(3\lambda_m + 2\mu_m)R^3 + 4c^3\mu_m} + \frac{R^3\alpha_m(3\lambda_m + 2\mu_m)}{(3\lambda_m + 2\mu_m)R^3 + 4c^3\mu_m}.$$

The remaining two constants can be presented as

$$A_1 = \frac{MP_{12} - QP_{22}}{P_{11}P_{22} - P_{12}P_{21}}, \quad A_2 = -\frac{MP_{11} - QP_{21}}{P_{11}P_{22} - P_{12}P_{21}}, \quad (4.14)$$

where the quantities $M, Q, P_{11}, P_{12}, P_{21}, P_{22}$ are explicitly given in Appendix (A).

5 Thermal expansion coefficient (CTE) expression

To obtain the effective thermal expansion coefficient α_{eff} for the composite sphere of Figure 1 we employ the following equation (Christensen, 2005)

$$\alpha_{eff} = \frac{V - V_0}{3V(T - T_0)}, \quad (5.1)$$

where $V - V_0$ is the change of the total volume of the composite sphere due to the temperature variation from $(T_0 - T)$. Since

$$V - V_0 = 4\pi R^2 u(R), \quad (5.2)$$

we obtain

$$\alpha_{eff} = \frac{u(R)}{R(T - T_0)}. \quad (5.3)$$

Substituting $u(R) = u^{(m)}(R)$ from equation (4.11), we determine the effective CTE as

$$\alpha_{eff} = \frac{C_1}{R^3} + C_2, \quad (5.4)$$

with constants C_1 and C_2 given by (4.13) and (4.14).

Introducing auxiliary quantities

$$\eta = \frac{b^3}{R^3}, \quad A = \frac{a}{b}, \quad \text{and} \quad \Gamma = \frac{c}{b}, \quad (5.5)$$

the effective coefficient of thermal expansion can be written in the following compact form

$$\begin{aligned} \alpha_{eff}(\eta) = & ((3\lambda_m + 2\mu_m)\alpha_m + 3(\lambda_m + 2\mu_m)\Theta_1(c)\bar{A}_1(\eta)\eta)F(\eta) + \\ & + \Gamma^3(3(\lambda_m + 2\mu_m)\Theta_2(c)\bar{A}_2(\eta) + \bar{k}_4)F(\eta)\eta. \end{aligned} \quad (5.6)$$

Here, function $F(\eta)$ is

$$F(\eta) = \frac{1}{4\Gamma^3\eta\mu_m + 3\lambda_m + 2\mu_m}, \quad (5.7)$$

and the coefficient

$$\bar{k}_4 = -(3\lambda_m + 2\mu_m)\alpha_m - (3\lambda_m + 6\mu_m)\left(\frac{\bar{j}_4}{\Gamma^\beta} - \bar{g}_3\right), \quad (5.8)$$

where

$$\bar{j}_4 = \frac{(\alpha_{ip} - \alpha_m)(3\lambda_{ip} - 3\lambda_m + 2\mu_{ip} - 2\mu_m)\Gamma^\beta}{((\lambda_{ip} - \lambda_m + 2\mu_{ip} - 2\mu_m)\beta - 3\lambda_{ip} + 3\lambda_m - 4\mu_{ip} + 4\mu_m)(\Gamma^\beta - 1)} \quad (5.9)$$

$$\bar{g}_3 = \frac{g_{31}\beta + g_{32} + \Gamma^\beta(g_{33}\beta + g_{34})}{(\Gamma^\beta - 1)g_{35}}, \quad (5.10)$$

where

$$\begin{aligned}
g_{31} &= 4 (\lambda_{ip} \mu_m - \mu_{ip} \lambda_m) \alpha_m + (3 \lambda_{ip}^2 + 8 \lambda_{ip} \mu_{ip} + 4 \mu_{ip}^2) \alpha_{ip} + \\
&+ (3 \lambda_m^2 - 2 (3 \lambda_{ip} + 2 \mu_{ip} - 4 \mu_m) \lambda_m + 4 \mu_m^2 - 4 (3 \lambda_{ip} + 2 \mu_{ip}) \mu_m) \alpha_{ip}, \\
g_{32} &= (6 (3 \lambda_{ip} + \mu_{ip} - 3 \mu_m) \lambda_m - 9 \lambda_m^2 - 8 \mu_m^2 + 12 (2 \lambda_{ip} + \mu_{ip}) \mu_m) \alpha_{ip} + \\
&+ (12 \mu_{ip} \lambda_m + 2 (-3 \lambda_{ip} + 2 \mu_{ip}) \mu_m - 6 \lambda_{ip} \mu_{ip} - 4 \mu_{ip}^2) \alpha_m + \\
&- (9 \lambda_{ip}^2 + 12 \lambda_{ip} \mu_{ip} + 4 \mu_{ip}^2) \alpha_{ip}, \\
g_{33} &= 4 (\lambda_{ip} \mu_m - \mu_{ip} \lambda_m) \alpha_{ip} - (3 \lambda_{ip}^2 + 8 \lambda_{ip} \mu_{ip} + 4 \mu_{ip}^2) \alpha_m + \\
&+ ((6 \lambda_{ip} + 12 \mu_{ip} - 8 \mu_m) \lambda_m - 3 \lambda_m^2 - 4 \mu_m^2 + 4 (\lambda_{ip} + 2 \mu_{ip}) \mu_m) \alpha_m, \\
g_{34} &= (6 (\mu_{ip} + \mu_m) \lambda_m + 4 \mu_m^2 - 4 (3 \lambda_{ip} + \mu_{ip}) \mu_m) \alpha_{ip} + \\
&+ (9 \lambda_m^2 - 6 (3 \lambda_{ip} + 4 \mu_{ip} - 2 \mu_m) \lambda_m + 4 \mu_m^2 - 6 (\lambda_{ip} + 2 \mu_{ip}) \mu_m) \alpha_m + \\
&+ (9 \lambda_{ip}^2 + 18 \lambda_{ip} \mu_{ip} + 8 \mu_{ip}^2) \alpha_m, \\
g_{35} &= (\lambda_{ip} + 2 \mu_{ip} - \lambda_m - 2 \mu_m) \beta - 2 \mu_{ip} + 2 \mu_m.
\end{aligned} \tag{5.11}$$

Furthermore, functions $\bar{A}_1(\eta)$ and $\bar{A}_2(\eta)$ are written using notations (5.5) as

$$\begin{aligned}
\bar{A}_1(\eta) &= -\frac{((m_1 + \eta m_2) p_{121} - \bar{Q} p_{221}) F(\eta) - m_3 p_{121} + p_{222} \bar{Q}}{(p_{121} p_{211} \eta - p_{111} p_{221}) F(\eta) + p_{111} p_{222} - p_{121} p_{212}}, \\
\bar{A}_2(\eta) &= \frac{((m_2 p_{111} - p_{211} \bar{Q}) \eta + m_1 p_{111}) F(\eta) - m_3 p_{111} + p_{212} \bar{Q}}{(p_{121} p_{211} \eta - p_{111} p_{221}) F(\eta) + p_{111} p_{222} - p_{121} p_{212}},
\end{aligned} \tag{5.12}$$

where quantities $m_1, m_2, m_3, \bar{Q}, p_{111}, p_{121}, p_{212}, p_{211}$ and p_{222} introduced in (5.12) are given in Appendix (B).

We note that in absence of the interphase zone, equation (5.6) reduces to the CTE expression for a two-phase composite containing isotropic spherical inclusions surrounded by an isotropic matrix as

$$\begin{aligned}
\alpha_{eff} &= \alpha_m + \\
&+ \frac{(\alpha_i - \alpha_m) (A^3 - 1) (3 K_m + 4 \mu_m) K_i \mu_i \eta}{((3 K_m + 4 \mu_i) A^3 K_i + 4 (K_m - K_i) \mu_i) \mu_m \eta + (3 (\mu_i - \mu_m) A^3 K_i - (3 K_i + 4 \mu_m) \mu_i) K_m}.
\end{aligned} \tag{5.13}$$

Here, K_i and K_m , are the bulk moduli for the inclusion and matrix materials, respectively.

Expression (5.13) is valid for hollow inclusion ($0 < A < 1$) and solid inclusion ($A = 0$) as given by Levin (1968). For the case of void, we have $A = 1$ and consequently $\alpha_{eff} = \alpha_m$.

6 Numerical results and discussion

In this section, we present and analyse several numerical examples. First, we investigate the exact thermo-elasticity solution obtained in Section 4 for hollow and solid inclusions, as well as voids, assuming a ceramic inclusion in a metallic matrix. Next, we analyse in detail the effect of geometric and physical parameters associated with the interphase zone on the coefficient of thermal expansion for different wall thicknesses in terms of the volumetric fraction ratio η .

The single sphere of the particulate composite is assumed to be made of metallic matrix (aluminium) containing ceramic inclusions (alumina), with the following thermo-elastic properties: $\lambda_i = 90$ GPa, $\mu_i = 124$ GPa, $\alpha_i = 8 \cdot 10^{-6} \text{ K}^{-1}$, $\lambda_m = 51$ GPa, $\mu_m = 26$ GPa, $\alpha_m = 2 \cdot 10^{-5} \text{ K}^{-1}$. We assume that the interphase zone is softer than the matrix material in order to simulate, for example, an imperfect interfacial adhesion between the phases or to model presence of pores or other microstructural defects, such as cracks, around the inclusion that occur as a consequence of the elastic mismatch between the metallic material of the matrix and the ceramic material of the inclusion. In accordance with (2.1), we assume the following properties of the interphase zone: $\lambda_{ip} = 36$ GPa, $\mu_{ip} = 19$ GPa, $\alpha_{ip} = 3 \cdot 10^{-5} \text{ K}^{-1}$.

From a geometric point of view, we consider the following cases: $a = 0$ (solid inclusion), $a/b = 0.8$ (hollow inclusion) and $a/b = 1$ (void) which will be shown in the figures with red, blue and black lines, respectively. Continuous (solid) lines are used for composite without the interphase zone, dashed lines for composites with the interphase zone. For the graded interphase zone, the value of the inhomogeneity parameter is taken as $\beta = 10$.

Figures 2a and 2b show the normalised Lamé modulus $\bar{\lambda}(r) = \lambda(r)/\lambda_i$ and the coefficient of thermal expansion $\bar{\alpha}(r) = \alpha(r)/\alpha_i$ as a function of the radial co-ordinate. Numerical results obtained in the presence of the interphase zone (dashed lines) are compared to the

two-phase model that is a homogeneous inclusion in a homogeneous matrix (continuous lines).

Figure 3 shows variation of the normalised radial displacement $\bar{u}_r = u_r / ((T - T_0) \alpha_i b)$ for two inclusion types: solid inclusions and hollow inclusions, both with and without the interphase zone. We observe an increase of the normalised radial displacement around the interface, due to the interphase material being softer than both matrix and inclusion materials, while in the inclusions a small decrease is observed, due the inclusion material being stiffer.

The normalised radial stress $\bar{\sigma}_r = \sigma_r / (3 (T - T_0) \alpha_i K_i)$ is shown in Fig. 4. We observe that the soft interphase zone leads to a reduction of radial stress in the inclusion; the reduction is more significant for the solid inclusion than for the hollow inclusion. In the interphase zone and in the matrix, this effect is similar for both types of inclusions.

The normalised hoop stress $\bar{\sigma}_\theta = \sigma_\theta / (3 (T - T_0) \alpha_i K_i)$ is presented in Fig. 5. We observe that the soft interphase zone increases the stress jump across the interface between the inclusion and the interphase zone, compared to a two-phase model without the interphase. A small decrease in stress values is observed in the inclusions.

Figure 6 shows normalised radial displacement $u^* = u_r / ((T - T_0) \alpha_m b)$ for the case of voids ($a/b = 1$). We note that this case is also related to a hollow graded inclusion embedded in a homogeneous matrix. Figure 7 shows normalised radial and hoop stresses that occur in the matrix, due to the presence of the graded interphase zone around the void. We observe that the compressive stress field has developed around the void when a composite is subjected to the uniform temperature rise (Hatta et al, 2000).

Now, the CTE expression (5.6) is studied numerically as a function of the volume fraction coefficient η , assuming values for the material properties of the homogeneous inclusion and matrix as before. The normalised CTE is calculated for solid inclusion ($A = 0$), hollow inclusions ($A = 0.9, A = 0.98$) and void ($A = 1$), all with and without the interphase zone. The cases without the interphase zones are obtained from equation (5.13) and the results are in agreement with those found in the literature (see, i.e. Figure 5 of Gusev, 2014).

For all cases with the interphase zone (dashed lines), we assume $c/b = 1.2$. We observe that the coefficient of thermal expansion increases significantly when the interphase zone is present, compared to a corresponding case without the interphase zone. This is due to the high adopted value of the CTE at the interface between the inclusion and the matrix. The increase becomes more significant as the wall thickness of the inclusion decreases.

7 Conclusions

In this paper, an exact expression for the coefficient of thermal expansion of a particular composite with spherical inclusions or voids is derived using a three-phase micro-mechanical model able to take into account the effect of graded interphase zone. The analytical solutions are obtained in closed form in the framework of the linear elasticity using hypergeometric functions. Comparative numerical investigations have revealed localised effects due to graded interphase zone, in terms of the thermo-elastic properties of the phases. This allowed us to quantify the role played by the wall thickness of the inclusions on the effective CTE.

Appendix

(A) The explicit form of the quantities M, Q, P_{ij} of section 4 are here written.

$$\begin{aligned}
M &= -\frac{3(\lambda_m + 2\mu_m)(3\lambda_m + 2\mu_m)R^3g_3}{R^3(3\lambda_m + 2\mu_m) + 4c^3\mu_m} + \frac{3R^3\alpha_m(3\lambda_m + 2\mu_m)(\lambda_m + 2\mu_m)}{R^3(3\lambda_m + 2\mu_m) + 4c^3\mu_m} \\
&\quad - \left(\frac{4\mu_m(3\lambda_m + 2\mu_m)c^{-\beta}(c^3 - R^3)}{R^3(3\lambda_m + 2\mu_m) + 4c^3\mu_m} + \frac{((\lambda_m + 2\mu_m)\beta - 3\lambda_m - 2\mu_m)(b^\beta c^{-\beta} - 1)}{b^\beta - c^\beta} \right) g_4, \\
Q &= -\frac{((3\lambda_{ip} + 2\mu_{ip} + 4\mu_i)(3\lambda_i + 2\mu_i)a^3 - 4\mu_i(3\lambda_i + 2\mu_i - 3\lambda_{ip} - 2\mu_{ip})b^3)g_3}{(3\lambda_i + 2\mu_i)a^3 + 4b^3\mu_i} + \\
&\quad + \left(\frac{4\mu_i(3\lambda_i + 2\mu_i)b^{-\beta}(a^3 - b^3)}{(3\lambda_i + 2\mu_i)a^3 + 4b^3\mu_i} + \frac{((\lambda_{ip} + 2\mu_{ip})\beta - 3\lambda_{ip} - 2\mu_{ip})(c^\beta b^{-\beta} - 1)}{b^\beta - c^\beta} \right) g_4 + \\
&\quad + \frac{3(3\lambda_i + 2\mu_i)a^3\alpha_i(\lambda_i + 2\mu_i)}{(3\lambda_i + 2\mu_i)a^3 + 4b^3\mu_i} - (3\lambda_i + 2\mu_i)\alpha_i + (3\lambda_{ip} + 2\mu_{ip})\alpha_{ip}, \\
P_{11} &= -\frac{(\lambda_{ip} + 2\mu_{ip})q_1\beta\Theta_3(b)}{b^3} + \\
&\quad + \frac{4((\mu_{ip} - \mu_i)(3\lambda_i + 2\mu_i)a^3 + \mu_i(3\lambda_i + 2\mu_i + 4\mu_{ip})b^3)\Theta_1(b)}{((3\lambda_i + 2\mu_i)a^3 + 4b^3\mu_i)b^3}, \\
P_{12} &= -(\lambda_{ip} + 2\mu_{ip})q_2\beta\Theta_4(b) + \\
&\quad - \frac{((3\lambda_{ip} + 4\mu_i + 2\mu_{ip})(3\lambda_i + 2\mu_i)a^3 - 4\mu_i(3\lambda_i - 3\lambda_{ip} + 2\mu_i - 2\mu_{ip})b^3)\Theta_2(b)}{(3\lambda_i + 2\mu_i)a^3 + 4b^3\mu_i}, \\
P_{21} &= \frac{12\mu_m(\lambda_m + 2\mu_m)\Theta_1(c)}{R^3(3\lambda_m + 2\mu_m) + 4c^3\mu_m} - \frac{(\lambda_m + 2\mu_m)(b^\beta c^{-\beta} - 1)q_1b^\beta\beta\Theta_3(c)}{c^3(b^\beta - c^\beta)}, \\
P_{22} &= -\frac{3(\lambda_m + 2\mu_m)(3\lambda_m + 2\mu_m)\Theta_2(c)R^3}{R^3(3\lambda_m + 2\mu_m) + 4c^3\mu_m} - \frac{(\lambda_m + 2\mu_m)(b^\beta c^{-\beta} - 1)q_2b^\beta\beta\Theta_4(c)}{b^\beta - c^\beta}.
\end{aligned} \tag{7.1}$$

(B) The quantities $m_1, m_2, m_3, \bar{Q}, p_{111}, p_{121}, p_{212}, p_{211}, p_{222}$, introduced in (5.12) of section 5, are written as

$$m_1 = -(3\lambda_m + 6\mu_m)(3\lambda_m + 2\mu_m)\bar{g}_3 + 3\alpha_m(3\lambda_m + 2\mu_m)(\lambda_m + 2\mu_m) + 4\mu_m(3\lambda_m + 2\mu_m)\frac{\bar{j}_4}{\Gamma^\beta}, \quad (7.2)$$

$$m_2 = -4\mu_m(3\lambda_m + 2\mu_m)\frac{\bar{j}_4}{\Gamma^{\beta-3}}, \quad m_3 = (\beta(\lambda_m + 2\mu_m) - 3\lambda_m - 2\mu_m)\frac{\bar{j}_4}{\Gamma^\beta},$$

and

$$\begin{aligned} \bar{Q} &= \frac{3(3\lambda_i + 2\mu_i)\alpha_i A^3(\lambda_i + 2\mu_i)}{A^3(3\lambda_i + 2\mu_i) + 4\mu_i} - \alpha_i(3\lambda_i + 2\mu_i) + \alpha_{ip}(3\lambda_{ip} + 2\mu_{ip}) + \\ &+ \left(\frac{4\mu_i(3\lambda_i + 2\mu_i)(A-1)(A^2 + A + 1)}{A^3(3\lambda_i + 2\mu_i) + 4\mu_i} - \beta(\lambda_{ip} + 2\mu_{ip}) + 3\lambda_{ip} + 2\mu_{ip} \right) \bar{j}_4 + \\ &- \frac{((3\lambda_{ip} + 4\mu_i + 2\mu_{ip})(3\lambda_i + 2\mu_i)A^3 - 4\mu_i(3\lambda_i - 3\lambda_{ip} + 2\mu_i - 2\mu_{ip}))\bar{g}_3}{A^3(3\lambda_i + 2\mu_i) + 4\mu_i}. \end{aligned} \quad (7.3)$$

and

$$\begin{aligned} p_{111} &= -(\lambda_{ip} + 2\mu_{ip})\bar{q}_1\beta\Theta_3(b) + \\ &- \frac{(4(\mu_i - \mu_{ip})(3\lambda_i + 2\mu_i)A^3 - 4\mu_i(3\lambda_i + 2\mu_i + 4\mu_{ip}))\Theta_1(b)}{A^3(3\lambda_i + 2\mu_i) + 4\mu_i}, \\ p_{121} &= -(\lambda_{ip} + 2\mu_{ip})\bar{q}_2\beta\Theta_4(b) + \\ &- \frac{((3\lambda_{ip} + 4\mu_i + 2\mu_{ip})(3\lambda_i + 2\mu_i)A^3 - 4\mu_i(3\lambda_i - 3\lambda_{ip} + 2\mu_i - 2\mu_{ip}))\Theta_2(b)}{A^3(3\lambda_i + 2\mu_i) + 4\mu_i}, \\ p_{212} &= \Gamma^{-\beta-3}(\lambda_m + 2\mu_m)\bar{q}_1\beta\Theta_3(c), \quad p_{211} = 12\mu_m(\lambda_m + 2\mu_m)\Theta_1(c), \\ p_{221} &= -3(\lambda_m + 2\mu_m)(3\lambda_m + 2\mu_m)\Theta_2(c), \quad p_{222} = \Gamma^{-\beta}(\lambda_m + 2\mu_m)\bar{q}_2\beta\Theta_4(c). \end{aligned} \quad (7.4)$$

and \bar{q}_1 and \bar{q}_2 , are

$$\begin{aligned} \bar{q}_1 &= \frac{4(\mu_{ip} - \mu_m)\Gamma^\beta}{(\beta + 3)(\Gamma^\beta(\lambda_m + 2\mu_m) - 2\mu_{ip} - \lambda_{ip})}, \\ \bar{q}_2 &= -\frac{(3\lambda_{ip} + 2\mu_{ip} - 3\lambda_m - 2\mu_m)\Gamma^\beta}{(\beta - 3)(\Gamma^\beta(\lambda_m + 2\mu_m) - 2\mu_{ip} - \lambda_{ip})}. \end{aligned} \quad (7.5)$$

We remark that $\Theta_i(b)$ and $\Theta_i(c)$ are independent from η .

Acknowledgements

Financial support of this research by the Royal Society of Edinburgh (UK) and the Italian Academy of Science under the International Exchanges Bilateral Programme is gratefully acknowledged.

References

- Anisimova, M., Knyazeva, A., Sevostianov, I. (2016) Effective thermal properties of an aluminum matrix composite with coated diamond inhomogeneities, *International Journal of Engineering Science* 106; 142-154.
- Christensen, R.M. (2005) *Mechanics of Composite Materials*. New York, Dover Publication.
- Erdelyi, A., Magnus, W., Oberhettinger, F., Tricomi, F.G. (1953) *Higher transcendental functions I*. McGraw-Hill Book Company, New York.
- Gusev, A.A. (2014) Effective coefficient of thermal expansion of n-layered composite sphere model: Exact solution and its finite element validation, *International Journal of Engineering Science* 84; 54-71.
- Hashin, Z. (1962) The elastic moduli of heterogenous materials, *Journal of Applied Mechanics* 29 (13); 143-150
- Hashin, Z. (1991) Thermoelastic properties of particulate composites with imperfect interface, *Journal of Mechanics of Physics and Solids* 39 (6); 745-762.
- Hatta, H., Takei, T., Taya, M. (2000) Effects of dispersed microvoids on thermal expansion behavior of composite materials, *Materials Science and Engineering A285*; 99-110.
- Herve E. (2002) Thermal and thermoelastic behaviour of multiply coated inclusion-reinforced composites. *International Journal of Solids and Structures* 39; 1041-58.
- Holliday, L., Robinson, J. (1973) Review: the thermal expansion of composites based on polymers, *Journal of Material Sciences* 8; 301-311.
- Kashtalyan, M., Menshykova, M. (2009) Effect of a functionally graded interlayer on three-dimensional elastic deformation of coated plates subjected to transverse loading. *Composite*

Structures 89; 167-176.

Kashtalyan, M., Menshykova, M., Guz, I.A. (2009) Use of a functionally graded interlayer to improve bonding in coated plates. *Journal of Adhesion Science and Technology* 23; 1591-1601.

Levin, V. M. (1968) On the coefficients of thermal expansion of heterogeneous materials. *Mehanika Tverdogo Tela* 2; 884.

Lombardo, N. (2005) Effect of an inhomogeneous interphase on the thermal expansion coefficient of a particulate composite, *Composites Science and Technology* 65; 2118-2128.

Lutz, M.P., Monteiro, P.J.M. and Zimmerman, R.W. (1997) Inhomogeneous interfacial transition zone model for the bulk modulus of mortar, *Cement and Concrete Research* 27(7); 1113-1122.

Lutz, M.P., Zimmerman, R.W. (1996) Effect of the interphase zone on the bulk modulus of a particulate composite, *Journal of Applied Mechanics* 63; 855-861.

Nemat-Nasser, S. and Hori, M. (1993) *Micromechanics: overall properties of heterogeneous solids*, Elsevier.

Sburlati, R., Cianci, R. (2015) Interphase zone effect on the spherically symmetric elastic response of a composite material reinforced by spherical inclusions, *International Journal of Solids and Structures* 71; 91-98.

Sburlati, R., Kashtalyan, M. (2016) Elasticity analysis of sandwich pipes with graded interlayers. *European Journal of Mechanics A/Solids* 59; 232-241.

Sburlati, R., Monetto, I. (2016) Effect of an inhomogeneous interphase zone on the bulk modulus of a particulate composite containing spherical inclusions, *Composites Part B: Engineering* 97; 309-316.

Sevostianov, I. (2007) Dependence of the effective thermal pressure coefficient of a particulate composite on particles size, *International Journal of Fracture* 145; 333-340.

Sevostianov, I., Kachanov, M. (2007) Effect of interphase layers on the overall elastic and

conductive properties of matrix composites. Applications to nanosize inclusion, *International Journal of Solids and Structures* 44; 1304-1315.

Sevostianov I., Kachanov, M. (2006) Homogeneization of a nanoparticle with graded interface, *International Journal of Fracture* 139:121-127.

Sevostianov I. (2011) On the thermal expansion of composite materials and cross-property connection between thermal expansion and thermal conductivity, *Mechanics of Materials* 45; 20-33.

Shen, L., Li, J. (2003) Effective elastic moduli of composites reinforced by particle or fiber with an inhomogeneous interface, *International Journal of Solids and Structures*, 40, 1393-1409.

Shen, L. and Li, J. (2005) Homogenization of a fibre/sphere with an inhomogeneous interphase for the effective elastic moduli of composites, *Proc. Roy. Soc. L.*, A-461; 1475-1504.

Sideridis, E., Papanicolaou, G.C. (1988) A theoretical model for the prediction of thermal expansion behavior of particulate composites, *Rheologica Acta* 27; 608-616.

Tagliavia, G., Porfiri, M., Gupta, N. (2010) Analysis of flexural properties of hollow-particle filled composites, *Composites: Part B* 41; 86-93.

Zappalorto, M., Salviato, M., Quaresimin, M. (2011) Influence of the interphase zone on the nanoparticle debonding stress, *Composites Science and Technology* 72; 49-55.

Zimmerman, R. W., Lutz, M.P. (1999), Thermal stresses and thermal expansion in a uniformly-heated functionally-graded cylinder, *Journal of Thermal Stresses*, vol. 22; 177-188.

Figure 1. Micro-mechanical model of the composite sphere

Figure 2. Thermo-elastic property distribution in the radial direction of the composite sphere (solid inclusion case)

Figure 3. Normalized radial displacement for solid and hollow inclusions with and without interphase zone

Figure 4. Normalized radial stress for solid and hollow inclusion with and without interphase zone

Figure 5. Normalized hoop stress for solid and hollow inclusion with and without interphase zone

Figure 6. Normalized radial displacement for a void of radius b with and without interphase zone in matrix

Figure 7. Normalized radial and hoop stress for a void with interphase zone in matrix

Figure 8. Behaviour of the normalized effective bulk modulus with and without interphase zone for different volumetric fractions

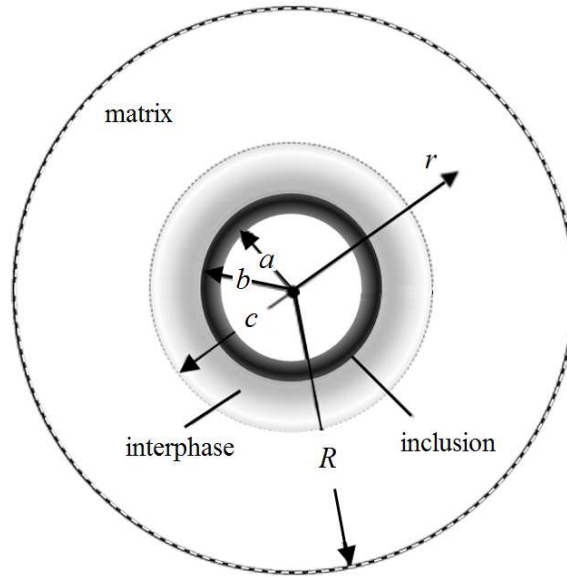


Figure 1: *Micro-mechanical model of the composite sphere*

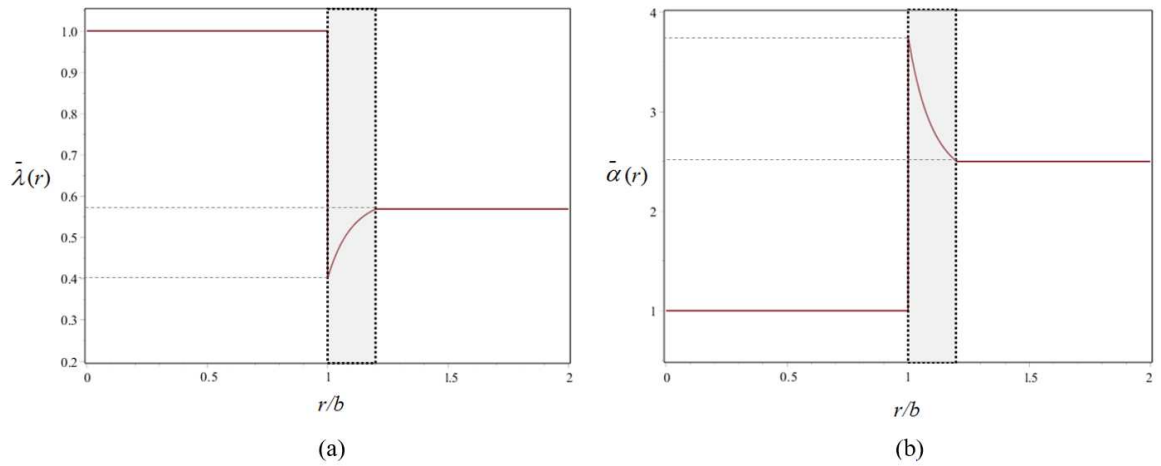


Figure 2: *Thermo-elastic property distribution in the radial direction of the composite sphere (solid inclusion)*

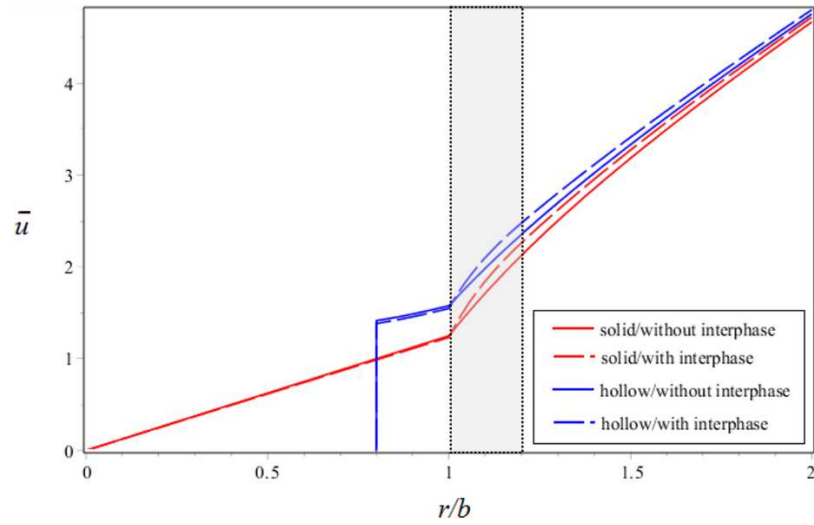


Figure 3: Normalized radial displacement for solid and hollow inclusions with and without interphase zone

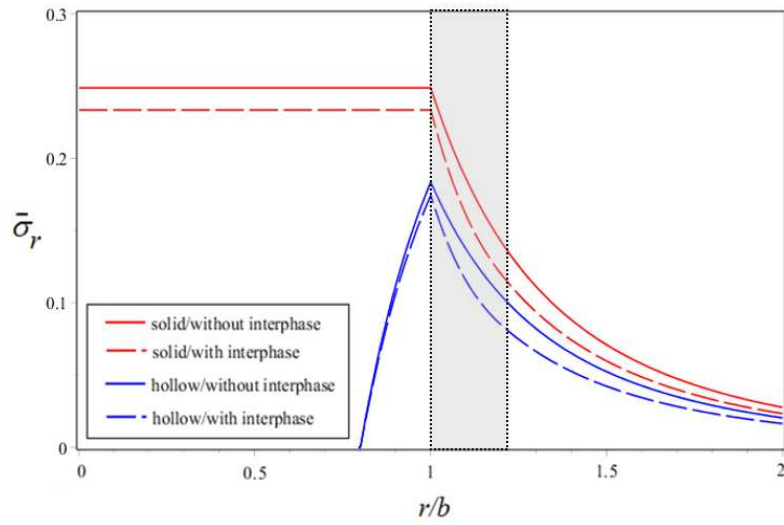


Figure 4: Normalized radial stress for solid and hollow inclusion with and without interphase zone

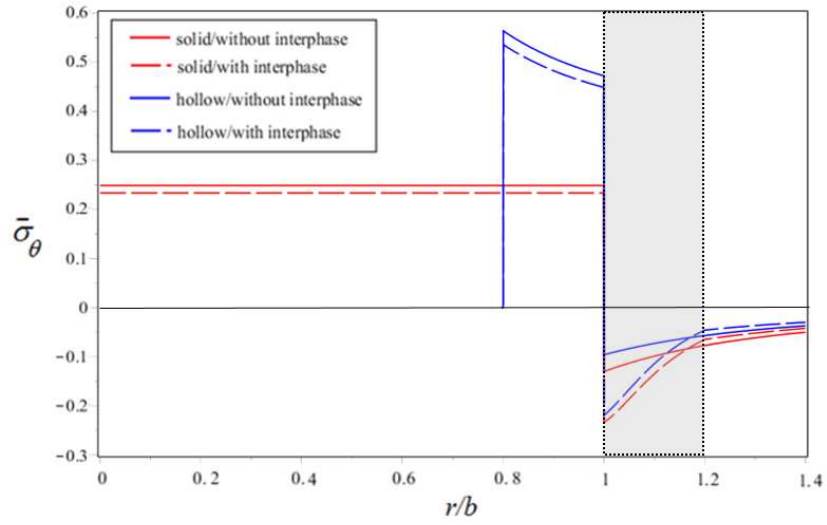


Figure 5: Normalized hoop stress for solid and hollow inclusion with and without interphase zone

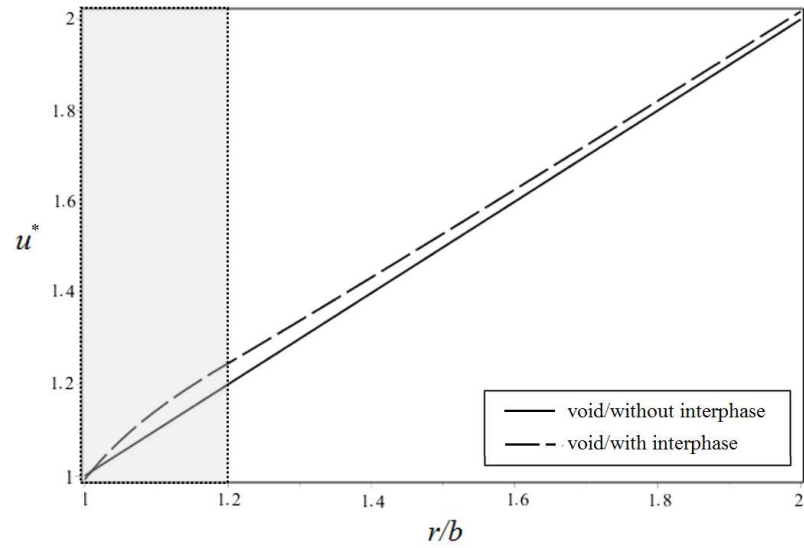


Figure 6: Normalized radial displacement for a void of radius b with and without interphase zone

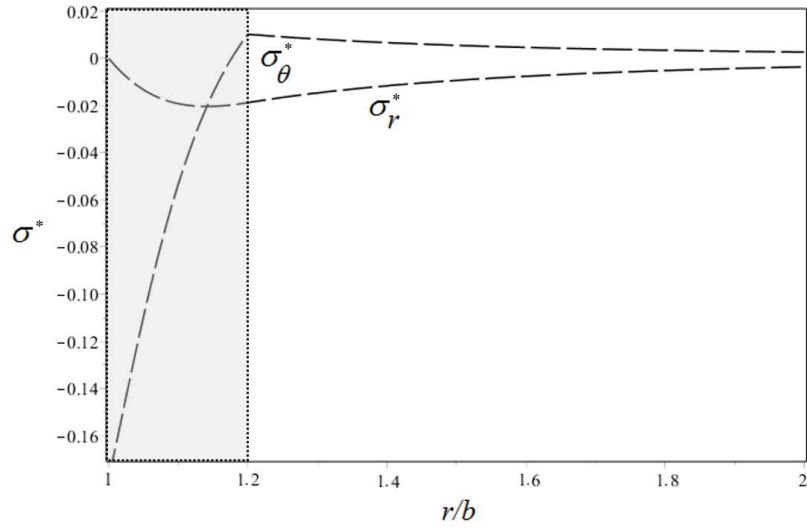


Figure 7: Normalized radial and hoop stress for a void with interphase zone

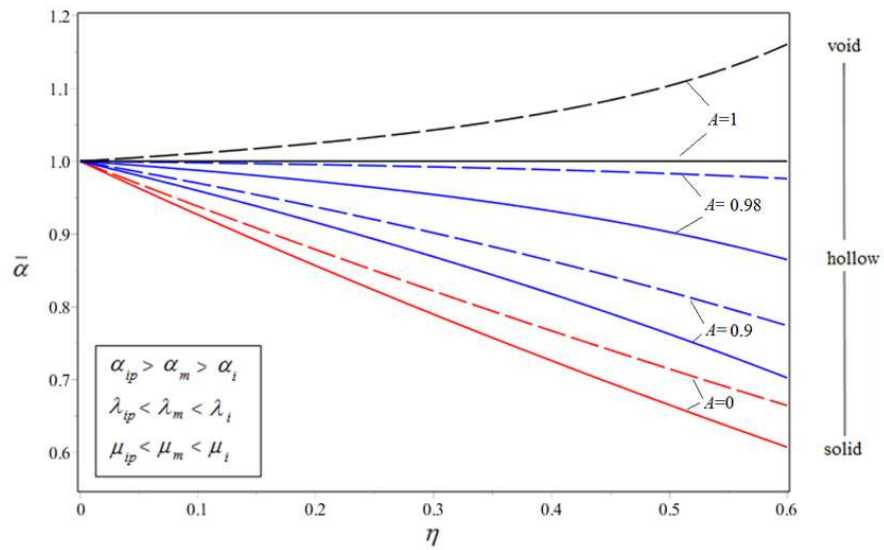


Figure 8: Behaviour of the normalized CTE with and without interphase zone for different volumetric fractions